K Channel Subconductance Levels Result from Heteromeric Pore Conformations

Mark L. Chapman and Antonius M.J. VanDongen

Department of Pharmacology and Cancer Biology, Duke University Medical Center, Durham, NC 27710

Voltage-gated K channels assemble from four identical subunits symmetrically arranged around a central permeation pathway. Each subunit harbors a voltage-sensing domain. The sigmoidal nature of the activation kinetics suggests that multiple sensors need to undergo a conformational change before the channel can open. Following activation, individual K channels alternate stochastically between two main permeation states, open and closed. This binary character of single channel behavior suggests the presence of a structure in the permeation pathway that can exist in only two conformations. However, single channel analysis of drk1 ($K_v2.1$) K channels demonstrated the existence of four additional, intermediate conductance levels. These short-lived subconductance levels are visited when the channel gate moves between the closed and fully open state. We have proposed that these sublevels arise from transient heteromeric pore conformations, in which some, but not all, subunits are in the "open" state. A minimal model based on this hypothesis relates specific subconductance states with the number of activated subunits (Chapman et al., 1997). To stringently test this hypothesis, we constructed a tandem dimer that links two K channel subunits with different activation thresholds. Activation of this dimer by strong depolarizations resulted in the characteristic binary open–close behavior. However, depolarizations to membrane potentials in between the activation thresholds of the two parents elicited highly unusual single channel gating, displaying frequent visits to two subconductance levels. The voltage dependence and kinetics of the small and large sublevels associate them with the activation of one and two subunits, respectively. The data therefore support the hypothesis that subconductance levels result from heteromeric pore conformations. In this model, both sensor movement and channel opening have a subunit basis and these processes are allosterically coupled.

The Journal of General Physiology

INTRODUCTION

Kinetic analyses of K currents in squid axon led Hodgkin and Huxley to propose a model for activation of voltage-gated channels in which four identical and independent charged particles need to translocate across the membrane to allow ion permeation (Hodgkin and Huxley, 1952). When voltage-gated ion channels were cloned several decades later, they were indeed found to consist of four domains or subunits, each containing a highly charged segment that traverses the membrane during activation (Yang and Horn, 1995; Larsson et al., 1996; Cha et al., 1999; Jiang et al., 2003). Models of voltage-dependent activation have become more complex, but most still assume that all four voltage sensors must move before channels can open (Sigworth, 1993; Bezanilla and Stefani, 1994; Zagotta et al., 1994). Studies of single channel behavior have shown that they alternate stochastically between two current levels, open and closed (Neher and Sakmann, 1976; Sigworth and Neher, 1980). The open and closed states must correspond to two distinct conformations of the permeation pathway. Crystal structures of bacterial K channels indeed reveal striking differences between the closed KcsA channel and the "opened" MthK channel (Doyle et al., 1998; Jiang et al., 2002), supporting the idea that the channel gate is formed by a cytoplasmic constriction (Armstrong, 1971; del Camino and Yellen, 2001). Recent experiments using soft-metal cysteine bridges in the *Shaker* K channel suggest that the structural differences between the open and closed channel may be much smaller, with a relatively narrow cytoplasmic constriction in both states (Webster et al., 2004).

The idea that channel gating is "binary" in nature is challenged by the occurrence of conductance levels that are intermediate between the closed and open state. Such subconductance levels (sublevels) can be observed in high-resolution recordings of many ion channels. In the drk1 ($K_v2.1$) K channel, short-lived sublevels were found to be associated with transitions between the closed and fully open state (Chapman et al., 1997). Because the K channel pore receives identical contributions from four subunits, we have suggested that the sublevels represent distinct heteromeric pore conformations, in which some but not all subunits are in a conformation that supports ion permeation (Fig. 1

Correspondence to A.M.J. VanDongen: vando005@mc.duke.edu

M.L. Chapman's present address is Icagen, Inc., 4222 Emperor Blvd., Durham, NC 27703.

Abbreviations used in this paper: COP, conditional open probability; FL, first latency; Po, open probability.

J. Gen. Physiol. © The Rockefeller University Press $8.00
Volume 126 Number 2 August 2005 87–103
http://www.jgp.org/cgi/doi/10.1085/jgp.200509253

A). It is important to critically test this hypothesis because it implies that gating and permeation are strictly coupled (VanDongen and Brown, 1989; VanDongen, 1992; Chapman et al., 1997; VanDongen, 2004b). Under standard recording conditions, most open–closed transitions appear smooth, with little evidence of visits to sublevels, which may be too short-lived to survive the inevitable low-pass filtering (Fig. 1, B–E). However, single channel recordings of large-conductance channels with very high time resolution revealed that open–closed transitions are not simple and smooth, but instead have a complex fine-structure (Fig. 1 B) characterized by visits to subconductance levels (Miodownik and Nonner, 1995; Shapovalov and Lester, 2004).

The heteromeric pore model (Fig. 1 A) is responsible for the intrinsic gating behavior of the channel (Fig. 1, F and G). In voltage-gated channels, this behavior is allosterically controlled by the movement of the voltage sensors. A minimal subunit-based model was proposed for voltage-gated K channels (Chapman et al., 1997), which represents a subset of the general allosteric model for a protein with four subunits and two tertiary states (Changeux and Edelstein, 1998). This model predicts that sublevels should be more prevalent when the channel is partially activated, which was confirmed for drk1 (Chapman et al., 1997). Activation-dependent sublevel behavior has also been demonstrated for the *Shaker* K channel (Zheng and Sigworth, 1997; Zheng and Sigworth, 1998), as well as for AMPA receptors (Rosenmund et al., 1998) and cGMP-gated channels (Taylor and Baylor, 1995).

Here we submit this subunit-subconductance hypothesis to a rigorous test, using a K channel in which individual subunits can be selectively activated. Subunit-specific activation was achieved by linking two subunits with different activation thresholds in a tandem-dimer construct (Krovetz et al., 1997; Chapman et al., 2001). If activation of all four subunits is required for channel opening, then dimeric K channels should only open following step depolarizations that exceed the highest activation threshold. The subunit-subconductance hypothesis, however, predicts that channel openings should be observed at membrane potentials in between the two thresholds. In addition, this channel activity should be dominated by visits to two subconductance levels, resulting from activation of the two low-threshold subunits. Furthermore, the voltage dependence and kinetics of the two sublevels and the open state should reflect the activation properties of the parent subunits.

MATERIALS AND METHODS

Molecular Biology

Mutagenesis was performed using polymerase chain reaction (PCR) and drk1 in the pBluescript plasmid vector. Oligonucleotides were designed using the OLIGO software (National Biosciences, Inc.). Mutagenesis of small restriction fragments was performed by the "Megaprimer" technique (Sarkar and Sommer, 1990). Mutated fragments were sequenced using a 7-deaza-GTP DNA sequencing kit (Amersham Biosciences). Plasmid DNA was linearized using the Not I restriction enzyme. Sense RNA was transcribed using T7 RNA polymerase. RNA was capped using m7Gppp(5′)G.

Construction of Dimers

Dimers were constructed using a SphI restriction site located at nucleotide 1700 in the COOH terminus of drk1 (amino acid 560). A novel drk1 construct was made by introducing an SphI restriction site 20 nucleotides upstream of the start codon, which maintains the reading frame at nucleotide 1700 and introduces four glycine residues. Digestion of this vector with SphI yielded a 1.7 kb fragment encoding amino acids 1–560. This fragment was ligated into a drk1 construct linearized with SphI to produce the tandem dimer. Ion selectivity and activation properties of the wild type–wild type dimer were indistinguishable from the wild-type subunit expressed as a homo-tetramer (Krovetz et al., 1997).

Electrophysiology

Oocyte preparation and cRNA injection were done as previously described (VanDongen et al., 1990). Defolliculated oocytes were placed in a recording chamber perfused with the following solution (concentrations in mM): 100 NaCl, 2 KCl, 1 $MgCl_2$, high-Na solution: 100 NaCl, 1 $MgCl_2$, 10 HEPES pH 7.2 with NaOH. K^+ currents were recorded using a commercial two-electrode voltage clamp amplifier (Warner Instruments). Oocytes were impaled with electrodes filled with 3 M KCl. The resistances of the current and voltage electrodes were 0.3–1.5 and 1.0–4.0 MOhm, respectively. Voltage pulse protocols and data acquisition were managed by PClamp hardware and software (Axon Instruments). Linear leak and capacitive currents were corrected using a P/4 protocol. Single channel currents were recorded from cell-attached patches on manually devitellinized oocytes as previously described (Chapman et al., 1997). Patch pipettes were fabricated from thin wall borosilicate (type 7740) capillaries (TW150F, WPI), Sylguard (Dow-Corning Corp.) coated and fire polished. Solutions were as follows (concentrations in mM): bath, 100 KCl, 60 KOH, 10 EGTA, 10 HEPES, 2 $MgCl_2$, pH 7.2 (HCl); pipette, 150 NMDG, 5 KCl, 5 KOH, 2 $MgCl_2$, 2 $CaCl_2$, 10 HEPES, pH 7.2(HCl). Data were acquired with an Axopatch 200 patch clamp amplifier, Digidata 1200 interface, and PClamp6 software (Axon Instruments Inc.). Currents were filtered at 1.5 kHz (−3 db, 4-pole Bessel filter), digitized at 5–10 kHz, and stored on computer hard disk for offline analysis. Linear leakage and capacitative currents were corrected using a smoothed average of empty traces.

Single Channel Analysis

Single channel behavior was idealized and statistically analyzed using the TRANSIT software (VanDongen, 1996, 2004a). Amplitude histograms were constructed as previously described (Chapman et al., 1997). Amplitude histograms of S-L dimer records always contained two intermediate open levels (referred to as Sub1 and Sub2) in addition to the fully open and closed states. Single channel records from the S-L dimer were therefore first idealized by the TRANSIT algorithm, and subsequently "interpreted" (VanDongen, 1996) by assigning each dwell level to one of four states: closed, Sub1, Sub2, or open. Ensemble averages were constructed by averaging idealized or interpreted traces. First latency distributions were constructed by collecting from each record the duration of the first closed time that preceded any openings. Conditional open probabilities were constructed by removing

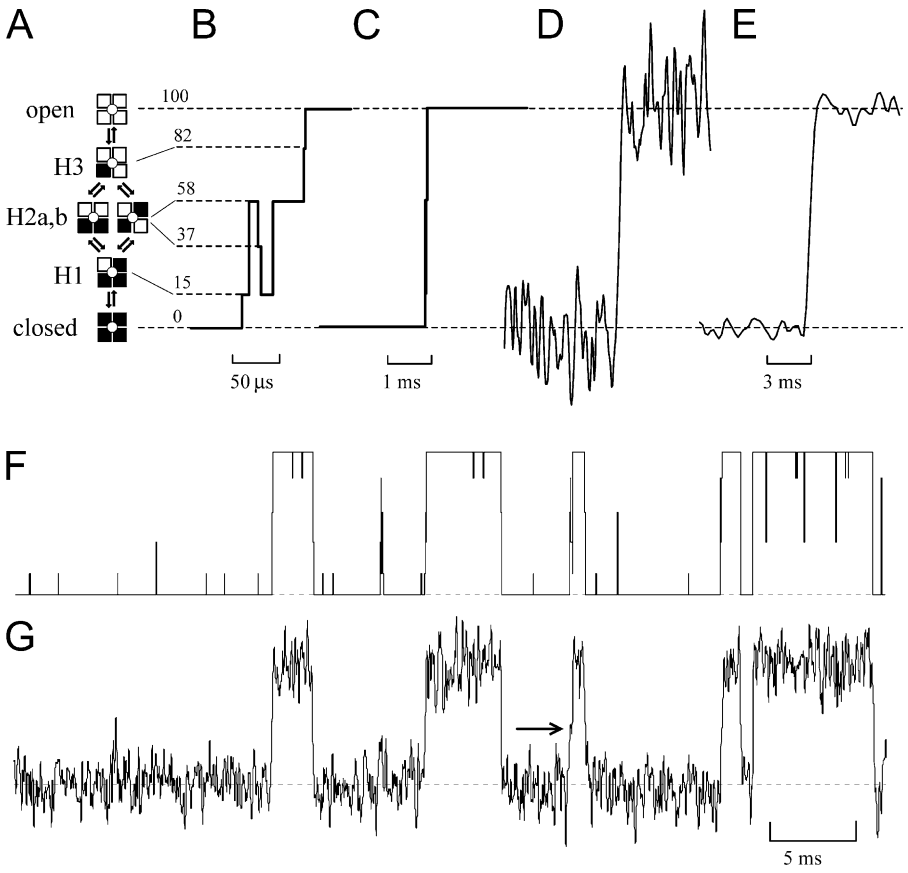

Figure 1. Heteromeric pore conformations and subconductance levels. (A) When ion channels move from the closed to the open state, a conformational change occurs in the pore. K channels consist of four identical subunits (indicated by squares in the model) surrounding a central pore. Each subunit makes an identical contribution to the lining of the permeation pathway. Therefore, when a K channel opens, each subunit must change its conformation from "closed" (black) to "open" (white). Consequently, as the channel moves between the homomeric open and closed states, it must visit heteromeric states (H1–H3), in which some subunits are "open" and others are "closed." Due to the tight packing of the subunits at the central pore region, it is likely that the transitions between the open and closed conformation are highly cooperative. Therefore, the heteromeric states H1–H3 are expected to be very short-lived. The permeation status of the heteromeric pore conformations is not immediately clear. It is conceivable that only the homomeric open state is capable of permeating ions. However, because subconductance levels (sublevels) were usually associated with transitions between the open and closed state in drk1, we have proposed that they arise from the heteromeric pore conformations H1–H3 (Chapman et al., 1997). Consistent with this idea, we have identified four distinct sublevels in drk1-L, a mutant with a large single channel conductance (Chapman et al., 1997). This subunit-subconductance hypothesis will be further tested in the remainder of this paper. (B) Single channel activity was simulated for the model shown in panel A using an approach described previously (VanDongen, 2004a). The rate constants leaving the fully open and closed states were set to 8,000 s^{-1}, while all other rate constants (leaving sublevels) were set to 32,000 s^{-1}. The amplitude levels for the subconductance states (H1–H3) were assigned values previously found for drk1-L (15, 37, 58, 82%). In this model, all gating transitions have a complex fine structure in which the channel visits at least three of the four subconductance levels. A representative opening transition is shown with high time resolution (and without noise or filtering), which follows the following itinerary: 0→15→58→37→15→58→82→100%. (C) The same transition as in B, on a slower (more realistic) timescale. Note the difference in scale bars. (D) The same transition as in C, after addition of Gaussian noise (standard deviation is 0.5 times the amplitude of the fully open state) and filtering (finite impulse response low-pass filter with a four-pole Bessel characteristic, cutoff frequency is 5 kHz). Note that the transition appears smooth. (E) An opening transitions taken from a single channel record of drk1 recorded in cell-attached mode at +40 mV. The record was low-pass filtered at 500 Hz. (F) The entire 50-ms record from which the transition in B–D was taken is shown without noise or filtering. (G) The same record as in F, with Gaussian noise added and after filtering (5 kHz). Note how most of the unsuccessful attempts to open or close that are seen in F do not survive the low-pass filter. Also, most of the complexity and fine-structure present in the opening and closing transitions is lost. However, occasionally a shoulder (arrow) can be observed, similar to those seen in wild-type drk1 (see Fig. 1 B in Chapman et al., 1997).

the first closed time from each record (by reassigning the zero time point to the beginning of the first opening) and averaging the time-shifted records.

Modeling

The open probability (Po), first latency (FL), and conditional open probability (COP) were estimated for each of the three conducting states identified (Sub1, Sub2, and open) at both 0 and +40 mV. This resulted in 18 curves that were fitted with various Markov models. Curves for Po(t), FL(t), and COP(t) were generated from of a set of differential equations corresponding to a specific model. These model curves were obtained by Euler integration using Microsoft Excel. Model parameters (rate constants, allosteric coefficients, and initial conditions for the COPs) were optimized by minimizing the sum of squared residuals (RSS) between the data and the model using the Solver function in Microsoft Excel.

RESULTS

The objective of the experiments described here is to test the hypothesis that K channel sublevels result from heteromeric pore conformations, in which some, but not all subunits support ion permeation (Fig. 1). The diagram shown in Fig. 1 A describes the intrinsic gating behavior of the channel under the hypothesis. It implies that open–close transitions are not all-or-nothing, as is usually assumed, but rather have a complex fine-

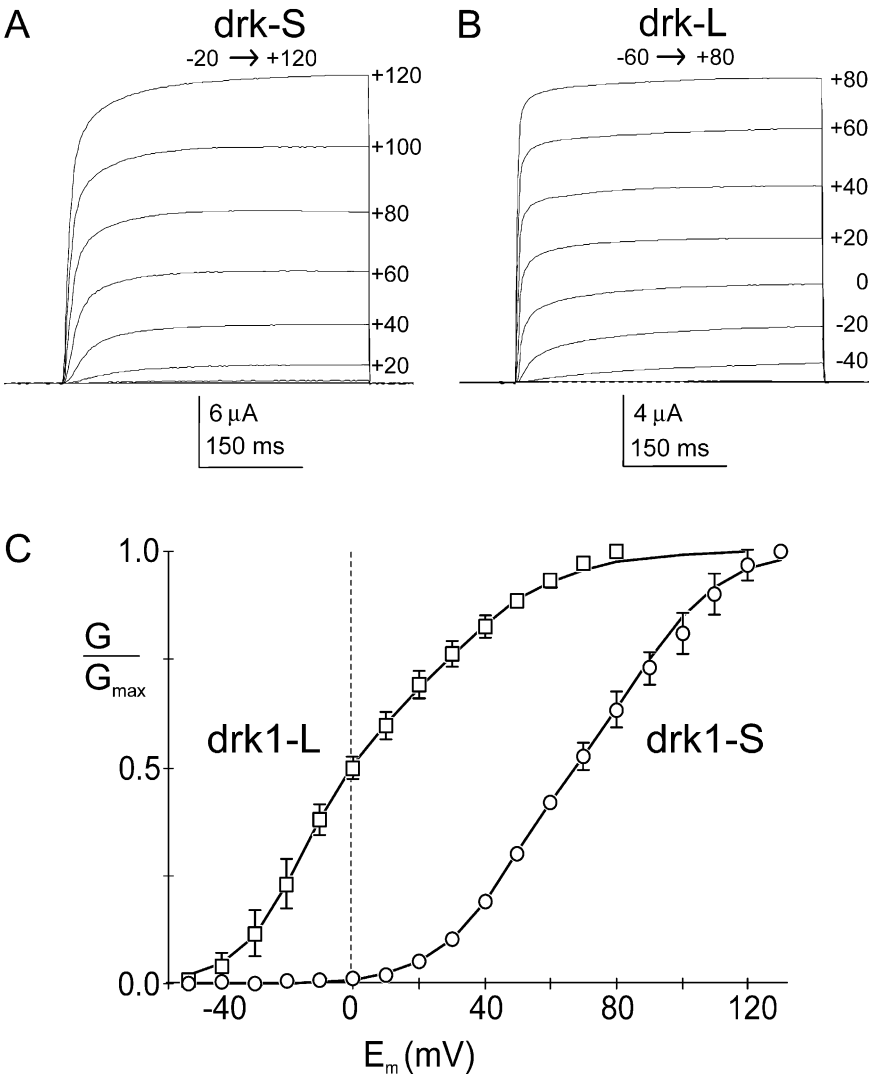

Figure 2. Drk1-S and drk1-L have widely different activation thresholds. Drk1-L (for "Large") is a previously described large-conductance mutant that has the same activation midpoint as drk1 (Chapman et al., 1997). Drk1-S (for "Shifted") was identified in a screen of S4 mutations: mutation of residues 289–292 from RRV(V) to LLV(A) resulted in a shift of the activation midpoint by +70 mV. (A and B) Families of outward K currents for drk1-S (A) and drk1-L (B) were elicited by 400-ms step depolarizations from a holding potential of −80 mV to membrane potentials indicated. (C) Comparison of the normalized conductance–voltage relationships for the two mutants used in this paper. Normalized conductances were calculated from whole cell current–voltage relationships (A and B), as previously described (VanDongen et al., 1990).

structure (Fig. 1 B), the details of which are destroyed by low-pass filtering under typical recording conditions (Fig. 1 D). However, due to the exponential nature of their lifetime distribution, unusually long-lived sublevels can occasionally occur and they may give rise to "shoulders" in open–close transitions (Fig. 1 G, arrow). Such shoulders were in fact observed in a small subset of openings in the drk1 K channel (Chapman et al., 1997). Additional support for the idea that channel openings are not all-or-nothing binary events has come from high-resolution, high-bandwidth recordings of large conductance ion channels, which also suggested that open–close transitions have a complex fine-structure (Miodownik and Nonner, 1995; Shapovalov and Lester, 2004). Fig. 1 G illustrates the open–close behavior of the channel as dictated by the heteromeric pore model in Fig. 1 A. In voltage-gated K channels, this intrinsic gating behavior is controlled by membrane potential, through the movement of the voltage sensors. K channels assemble from four identical subunits, each containing a sensor and each making a contribution to a structure in the permeation pathway that controls channel opening (Fig. 1 A).

To have more control over the activation of individual subunits, a dimer was constructed from two drk1 subunits with widely different activation thresholds. The first subunit of this dimer encodes an S4 mutant, drk1-S, in which the midpoint of activation is right shifted by 70 mV (Fig. 2, A and C). The second subunit in the dimer is a previously described mutant, drk1-L, with a large single channel conductance but normal activation midpoint (Fig. 2, B and C). Note that a membrane potential of 0 mV represents the threshold for activation of drk1-S and the activation midpoint for drk1-L. After correction for the shift in activation midpoint, the kinetics of activation for drk1-S and drk1-L are comparable (Fig. 2, A and B).

Single channel behavior of the two parent channels is characteristic of voltage-gated K channels (Fig. 3). Visits to stable, well-resolved sublevels were rare in ei-

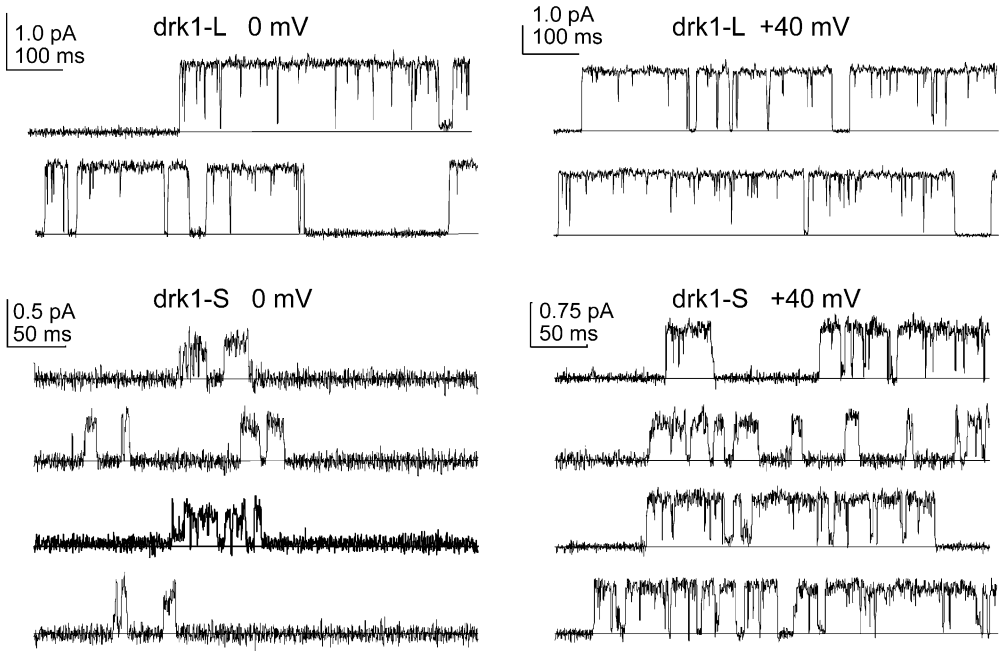

Figure 3. Single channel behavior of the parent channels drk1-S and drk1-L. Examples of single channel traces recorded in cell-attached patches for drk1-S and drk1-L, for step depolarizations to 0 and +40 mV. Traces for drk1-S at 0 mV were selected from several hundred records, in most of which the channel failed to open. Because of the very low open probability for drk1-S at 0 mV, it was not possible to estimate the number of channels in the patch. Due to the difference in single channel conductance, records for drk1-S (9 pS) are noisier than those for drk1-L (38 pS).

ther of the parent channels (as they are in drk1), and sublevels did not contribute a significant component to amplitude histograms (unpublished data). Due to the large shift in activation threshold, drk1-S channels are very reluctant to open at 0 mV. In fact, for the majority of traces, no openings were observed at all. Fig. 3 C illustrates a few traces where drk1-S did open and the single channel behavior appears normal and resembles that of drk1 at threshold. Ensemble averages were constructed for both drk1-S and drk1-L at 0 mV (Fig. 4). Whereas the open probability for drk1-S increases slowly and reaches a steady-state value of only 2.4 percent, drk1-L activates quickly and attains a steady-state open probability of 65%. Activation time constants were 6.12 ms and 113 ms for drk1-L and drk1-S, respectively (Fig. 4). At +40 mV, drk1-S attains an open probability of 40% (unpublished data), similar to that of wild-type drk1.

To test the heteromeric pore hypothesis illustrated in Fig. 1, a subunit-based kinetic model was generated for channels assembled from the S-L dimer (Fig. 5). We have previously proposed a minimal model, in which there are two conformational changes in each subunit: voltage sensor movement (Resting↔Active) and channel opening (Closed↔Open). The simplest possible way to couple them is in a linear three-state scheme: Resting↔Active/Closed↔Open. Fig. 5 A illustrates this model for the S and L subunits. A model describing tetrameric channels formed by the S-L dimer is then constructed by combining 2 S and 2 L subunits in an SLSL stoichiometry (Fig. 5, B–D). The complete model has a complex three-dimensional structure, due to the fact that the S and L subunits may activate in parallel. However, the 15-state triangular model has the same structure as the one proposed previously for a homotetrameric channel (Chapman et al., 1997), but it produces very different single channel behavior, in particular at membrane potentials between the activation thresholds of the L and S subunits. At these inter-

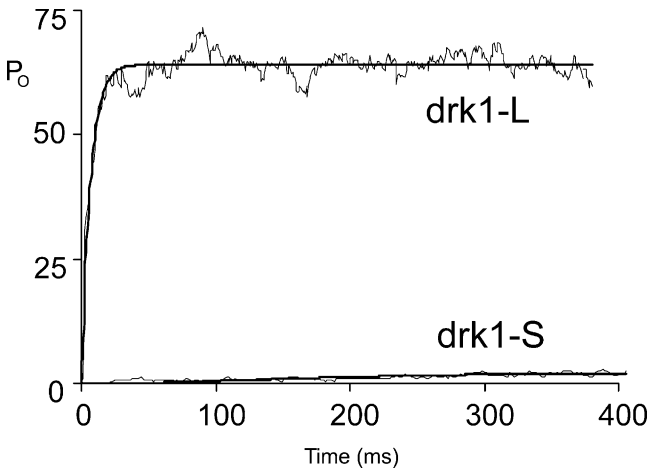

Figure 4. Ensemble averages for drk1-L and drk1-S. Probability of being open following a step depolarization to 0 mV in patches containing N channels (NP_O), where N = 1 for drk1-L, and N ≥ 1 for drk1-S (see Fig. 3). NP_O was obtained from ensemble averages after records were idealized by the TRANSIT algorithm (VanDongen, 1996, 2004a). Ensemble averages (thin line) were fit with the following model modified after Hodgkin and Huxley (1952): $P_O(t) = n_{inf} * [1 - \exp(-t/\tau_n)]^Q$. n_{inf} is the steady-state open probability, τ_n is the activation time constant, and (Q) is the exponent. The thick line illustrates the optimal fit. Optimized parameters were as follows: for drk1-L: τ_n = 6.29 ms, n_{inf} = 0.641, Q = 1.05, and for drk1-S: τ_n = 112.0 ms, n_{inf} = 0.024, Q = 1.00.

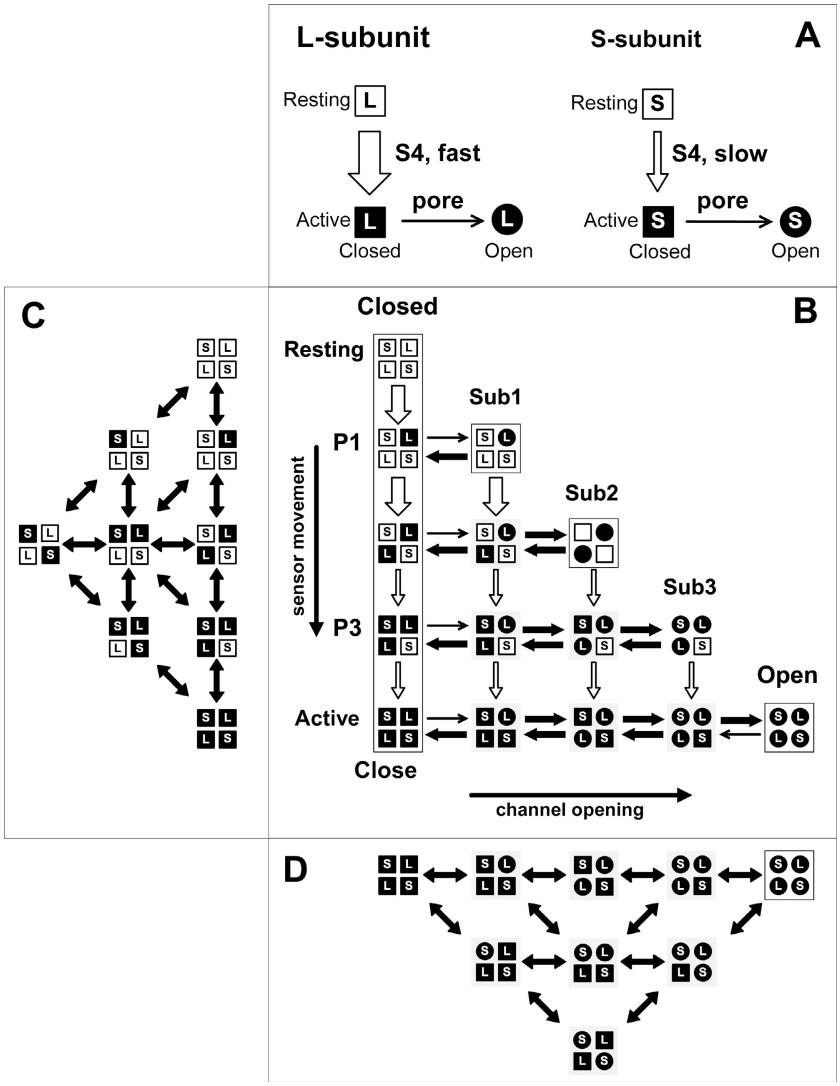

Figure 5. Subunit-subconductance model for voltage-gated K channels. The open↔close behavior illustrated in Fig. 1 G reflects the intrinsic kinetic properties of the gate, as described by the model in Fig. 1 A. In voltage-gated channels, this intrinsic gating behavior is allosterically controlled by membrane potential. A subunit-based kinetic scheme for K channels assembled from two S and two L subunits is constructed as follows. (A) The drk1-S and drk1-L subunits are modeled separately, since they differ in their voltage dependence. As before, each subunit is described by a linear three-state model that directly couples voltage sensor movement to channel opening. Closed states are represented by squares, open states by circles. Open squares indicate a resting voltage sensor; filled squares/circles imply the sensor has moved. The direction of the arrows specifies the position of the equilibrium and the width of the arrow the relative magnitude of the rate constants. The direction and width of the arrows are reflective of a membrane potential of 0 mV. Open arrows are voltage dependent (and involve sensor movements), closed arrows are voltage independent (indicating open–close gating transitions). (B–D) Combining two S and two L subunits in an S-L-S-L configuration results in a complex three-dimensional 36-state model. However, at intermediate membrane potentials, S-L channels will preferentially visit a subset of states, because the L subunits are likely to activate before the S subunits. The preferred itinerary is shown by the 15-state triangular model in B, while C and D illustrate all possible activation and opening transitions, respectively. The 15-state model contains three functionally homomeric states, at the corners of the triangle. Voltage sensor movements are represented by vertical transitions, open–close transitions by horizontal arrows. Rows labeled P1–P3 indicate partially activated channels, Columns H1–H3 represent the heteromeric pore conformations that are proposed to produce subconductance levels (Fig. 1 A). Highly unstable states are shown on a gray background: these are the heteromeric pore states that are connected by two wide filled arrows to neighboring states. Heteromeric pore states labeled Sub1, Sub2, and Sub3 are not as unstable as the remaining states in H1–H3, because channels in these states can only exit to the left. Sub1 and Sub2 are boxed to indicate that they are expected to predominate at membrane potentials below the activation threshold of the S subunits. At a negative holding potential, channels accumulate in the homomeric resting state. Following a step depolarization to 0 mV, they are expected to migrate downward and to the right. Because the two S subunits only activate slowly and reluctantly at this membrane potential (Fig. 4), channels will spend a relatively long time at the row labeled P2, before moving slowly to the bottom row.

mediate potentials, the two S subunits should be very reluctant to activate, forcing the channel to spend most of its time in the partially activated states indicated by rows P1 and P2 in Fig. 5 B. Therefore, the only types of openings possible are to the two sublevels labeled Sub1 and Sub2. A number of very specific (and highly unusual) predictions can be made from the model in Fig. 5 B. At potentials below the activation threshold of the S subunits, openings should be dominated by visits to two sublevels corresponding to Sub1 and Sub2. The latency until first opening should be fast for Sub1, somewhat slower and more sigmoidal for Sub2, and significantly slower for Open, since reaching it requires movement of the two reluctant voltage sensors in the S subunits. Furthermore, the probability of being in Sub1 and Sub2 should decline after reaching a maximum, since the channel will eventually move on to reach the open state. These predictions were tested by analyzing single channel behavior generated by S-L dimer K channels.

Expression of the S-L dimer construct resulted in functional K channels, which are predicted to be formed by the coassembly of two dimers resulting in an S-L-S-L stoichiometry. These S-L dimer K channels therefore should contain two S subunits, which have a

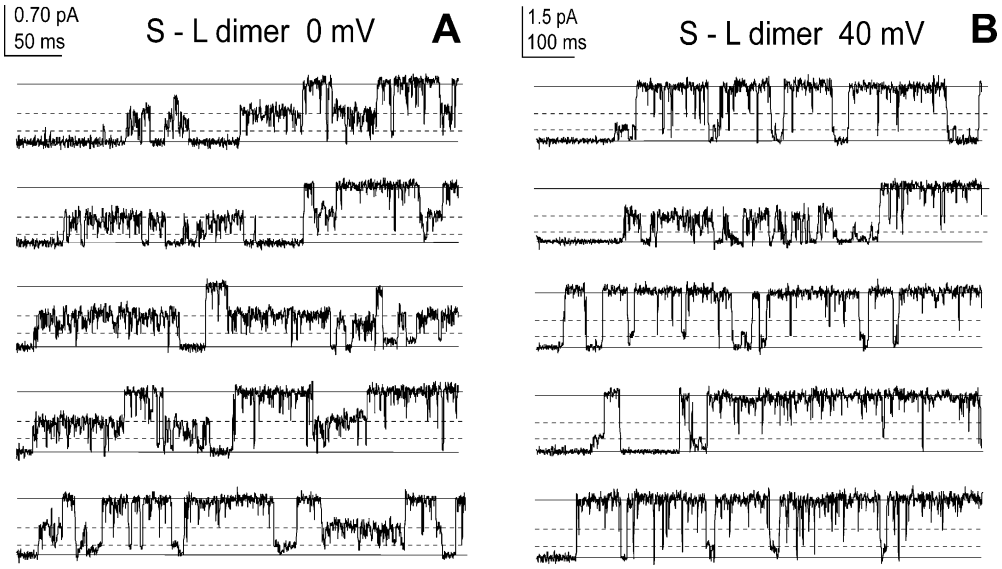

Figure 6. Single channel characteristics of the channel formed by the S-L dimer. (A and B) Single channel records of K channels expressed from the S-L dimer were recorded in cell-attached patches. Channels were activated by 750-ms step depolarizations to 0 and +40 mV. At 0 mV, early openings are dominated by visits to two sublevels, indicated by dotted lines. At +40 mV, sublevel visits become much more rare, although occasionally (e.g., record 2) persistent sublevel behavior can still be observed. The amplitude levels of Sub1 and Sub2 (see Fig. 7) are indicated by dotted lines.

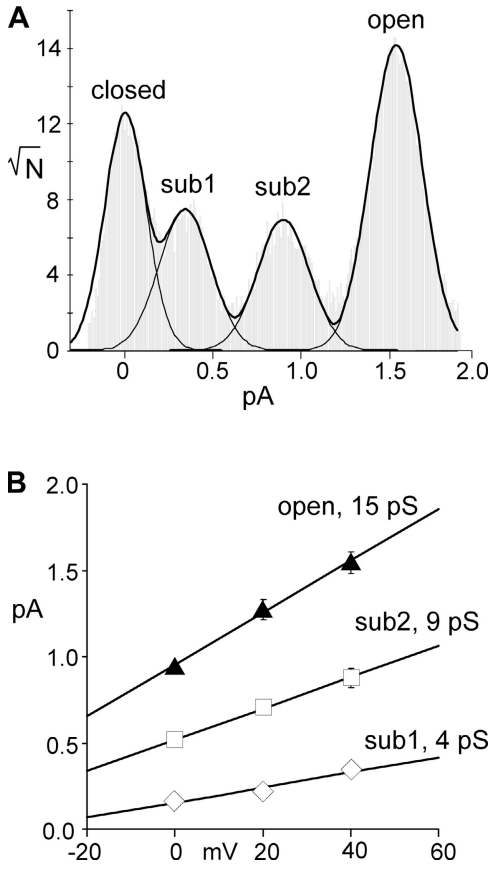

Figure 7. The S-L dimer channel has two subconductance levels. (A) Raw amplitude histograms were constructed and fitted with sums of Gaussian components as previously described (Chapman et al., 1997). Current levels arising from transitions (as judged by their slope) were omitted. At all potentials studied, four Gaussians were required; in addition to the fully open and closed level there were two well-resolved sublevels (Sub1 and Sub2). (B) Conductances were estimated by plotting the single channel amplitudes versus membrane potential, resulting in values of 4 pS, 9 pS, and 15 pS for the Sub1, Sub2, and the fully open state, respectively. The 4 pS and 9 pS values are similar to the 15% and 37% subconductance levels reported previously for drk1-L at threshold (Chapman et al., 1997).

low probability of being open at a membrane potential of 0 mV, and two L subunits, which are ~30-fold more likely to be open at the same potential (Fig. 4). S-L dimer channels opened readily at 0 mV, demonstrating that the S subunits did not behave as dominant negative regulators of voltage sensitivity. However, the single channel behavior was highly unusual, being dominated by visits to two subconductance levels (Fig. 6 A). At a more depolarized potential, where both S and L subunits would be effectively activated, single channel activity was more often characterized by the characteristic binary switching between the fully open and closed states (Fig. 6 B). Analysis of amplitude histograms of these recordings revealed the presence of two well-resolved subconductance levels, referred to as Sub1 (4 pS) and Sub2 (9 pS), in addition to the fully open state (15 pS) and closed state (Fig. 7). The single channel conductances of Sub1 and Sub2 were indistinguishable from the 15% and 37% subconductance levels reported previously (Chapman et al., 1997) for drk1-L recorded at threshold of activation. According to the scheme in Fig. 5 B, S-L dimer channels may also be able to visit a third sublevel (Sub3) when both L and one S subunit have activated. However, the amplitude histogram analysis did not reveal a significant fifth component corresponding to Sub3. Possible explanations for this finding are that the Sub3 levels is visited too infrequently, its lifetime is too short, or its amplitude is too close to the fully open state.

An important question is whether K channels formed following expression of the S-L dimer indeed have an

TABLE I

Current Amplitude Analysis of Individual Patches

				Relative Area		
Patch #	Open (pA)	sub1 (%)	sub2 (%)	O (%)	sub1 (%)	sub2 (%)
1	0.94	16	64	26.9	19.6	16.3
2	1.01	21	61	52.4	10.5	8.8
3	1.08	12	61	47.9	3.9	7.1
4	0.96	15	58	53.0	9.5	9.2
5	0.92	23	59	32.7	5.7	10.1
6	0.91	13	58	48.8	13.8	13.5
7	0.87	11	52	46.8	16.7	9.1
8	0.97	15	56	41.1	18.6	7.9
9	1.08	16	56	36.7	8.6	14.3
10	0.92	23	59	42.4	11.5	10.7
mean	**0.97**	**16**	**58**	**43**	**12**	**11**
SEM	0.02	1.2	1.0	2.6	1.6	0.9

All-point amplitude histograms of 10 individual patches were fitted with sum of two to five Gaussian components by maximizing the log likelihood, as previously described (Chapman et al., 1997). In each case, a sum of four Gaussians best described the amplitude distribution, indicating the presence of two sublevels in each recording. The table lists the current through the fully open state, as well as the normalized conductances of the two sublevels. In addition, the relative areas for the three open states are listed.

S-L-S-L stoichiometry. Several tandem dimer constructs of Kv2.1 have been previously described whose functional properties were consistent with their predicted stoichiometry (Krovetz et al., 1997; Chapman et al., 2001). In addition, it was found that incorporation of a lethal subunit in either the front or back half of a dimer results in nonfunctional channels (unpublished data), indicating that both parts of the dimer are incorporated in the final tetramer. Finally, Table I illustrates the results from fitting the all-point amplitude histogram with sums of Gaussians for 10 individual patches. In each case, there were two additional intermediate components (sublevels) in addition to the closed and fully open state. The amplitude of the fully open state, as well as the normalized conductances and relative areas of the two sublevels were similar from patch to patch, indicating that the dimers assemble in a consistent manner.

To investigate whether Sub1 and Sub2 indeed resulted from activation of one and two L subunits, respectively, their voltage dependence and kinetics were analyzed. Ensemble averages at a membrane potential of 0 mV showed that the probability of being in a sublevel rose rapidly to >30% and then slowly declined (Fig. 8 A). The probability of being in the fully open state increased more slowly, taking almost the entire 700-ms record to reach steady state. At +40 mV, the relative contribution of the subconductance levels was greatly reduced (Fig. 8 B). This analysis confirmed what can be seen qualitatively from the single channel traces. At 0 mV, sublevels prevailed early in the record,

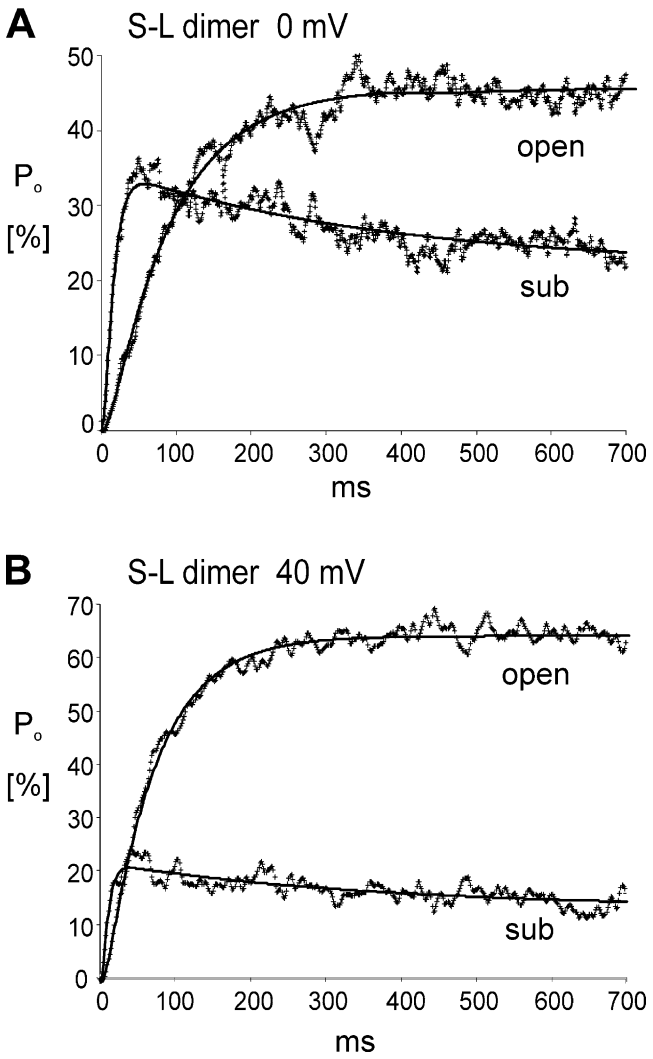

Figure 8. Activation kinetics of sublevels and the fully open state in the S-L dimer. (A and B) Probabilities of being in the fully open state or a subconductance level as a function of time after the step depolarization at both 0 and +40 mV were estimated by ensemble averages following idealization and interpretation by TRANSIT (VanDongen, 1996). The Po curves were fitted with a sum of three exponentials plus a constant (a_0), shown by the solid line. Po (t) = $a_0 + a_1 * \exp(-t/\tau_1) + a_2 * \exp(-t/\tau_2) + a_3 * \exp(-t/\tau_3)$. The optimal values in the format a_0, τ_1 (a_1), τ_2 (a_2), τ_3 (a_3) were as follows: for sublevels at 0 mV, 21.8, 367 (13,3), 8.48 (−3813), 8.40 (3777); for the open state at 0 mV, 45, 11.3 (7.4), 81.4 (16.7), 84.4 (−69.8); for sublevels at +40 mV, 13.1, 365 (8.6), 5.40 (−3812), 5.36 (3790); for the open state at +40 mV, 63.8, 9.3 (15), 58.7 (1.0), 60.7 (−79.8). Time constants (τ_1–τ_3) are in ms, their amplitudes (a_1–a_3) in percentages.

when the L subunits, but not the S subunits, are expected to be activated. At +40 mV, where all four subunits more readily activate, the single channel behavior is normalized.

Fig. 9 further delineates the activation characteristics of the two sublevels and the fully open state at a membrane potential of 0 mV. Sub1 activated rapidly with almost no delay, while Sub2 activated slower and showed

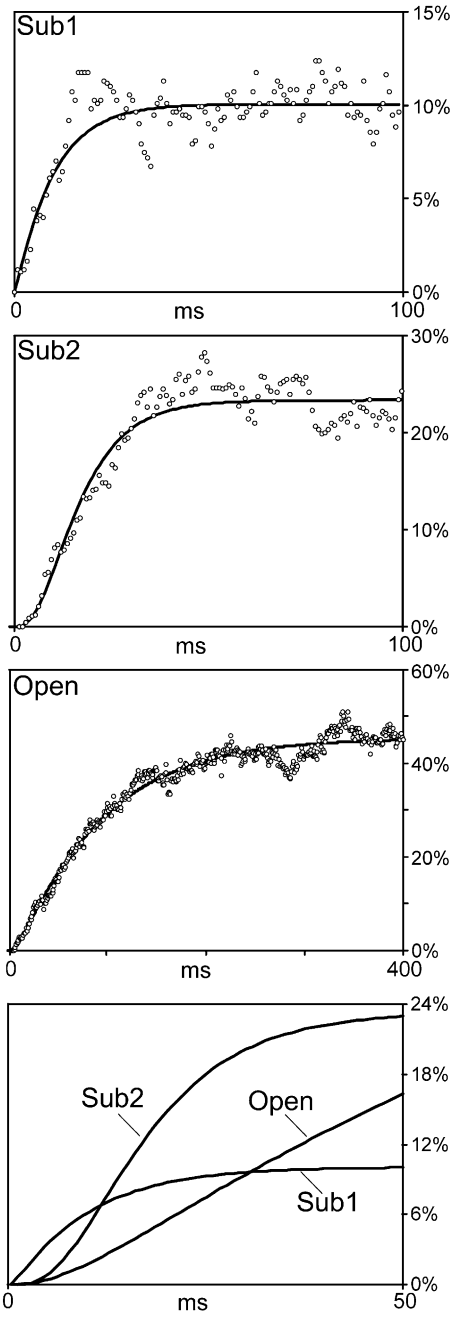

Figure 9. Activation kinetics of the three conductance levels in the S-L dimer. (A) Probabilities of being in each of the three conducting states (Sub1, Sub2, and Open) were calculated from ensemble averages of idealized and "interpreted" single channel data (see MATERIALS AND METHODS). Shown here are the probabilities of being in each state as a function of time following a step depolarization to 0 mV. These curves were fit with the following model: $P_{sub1}(t) = n_L(t)$, $P_{sub2}(t) = n_L^Q(t)$ and $P_{open}(t) = n_L^Q(t) * n_S^R(t)$, where $n_L^Q(t) = n_{inf,L}[1 - \exp(-t / \tau_L)]^Q$ and $n_S^R(t) = n_{inf,S}[1 - \exp(-t/\tau_S)]^R$. The model is derived on the Hodgkin and Huxley equations describing the change in normalized K conductance as a function of time following a step depolarization: $n(t) = n_{inf}[1 - \exp(-t/\tau)]^4$, where n_{inf} is the steady-state value and τ the activation time constant. The HH model assumes that four identical and independent charged particles must move before the channel can open, resulting in an exponent of 4. Our model assumes that activation of Sub1, Sub2, and Open requires movement of 1 L sensor, 2 L sensors, and 2 L + 2 S sensors, respectively. If the sensors move independently and do not display cooperativity, then both exponents Q and R should have a value of 2. Cooperativity between the sensor movements would result in deviations from these integer values. By optimizing the exponents (Q) and (R), our model allows for cooperativity between the movements of the voltage sensors. The optimal parameters values were: $\tau_L = 10.3$ ms, $\tau_S = 101.6$ ms, $n_{inf,L} = 0.22$, $n_{inf,S} = 0.47$, (Q) = 2.47, and R = 1.0.

a pronounced sigmoidicity. Activation of the fully open state was much slower, reaching half maximum only after Sub1 and Sub2 have completely activated. The three open probability curves for Sub1, Sub2, and Open could be well described with equations derived from the classical Hodgkin and Huxley model for activation of the K conductance in squid axon (Fig. 9). These curve fits resulted in estimates of activation time constants for the L and S subunit of 10.3 and 103 ms, respectively, which are similar to the 6- and 113-ms values for the parents.

The ensemble average can be dissected into two components: the waiting time until the first opening (first latency) and the conditional open probability (Aldrich et al., 1983). First latency distributions reflect all the voltage-dependent conformational changes in the activation pathway that occur following a step depolarization, leading up to channel opening. The movement of the voltage sensors is an important determinant of this waiting time. In the 15-state model based on the subunit-subconductance hypothesis (Fig. 5 B), entry into sublevels is reflective of activation, with visits to Sub1, Sub 2, and Open requiring the activation of one L subunit, two L subunits, and all four subunits, respectively. These differences should be borne out by the first latencies, which was indeed the case as Sub1 had the shortest latency, while the waiting time to reach the fully open state was the longest (Fig. 10). Sub2 had an intermediate latency, again with a more pronounced sigmoidal character. This difference in time course and sigmoidicity suggests that movement of a single voltage sensor is sufficient to activate Sub1, whereas movement of two sensors is required for activation of Sub2. The fact that the latency for the fully open state was significantly longer than those for Sub1 or Sub2 suggests that movement of the reluctant S-sensors is required for complete channel opening.

The conditional open probability (COP) describes what happens after an open state (or sublevel) is visited for the first time. At 0 mV, the COPs for Sub1 and Sub2 monotonically decline from a starting value of 40% and 45%, to a value <10% (Fig. 11). Because the drk1 K channel shows no significant inactivation on this timescale, the transient nature of these COPs implies that

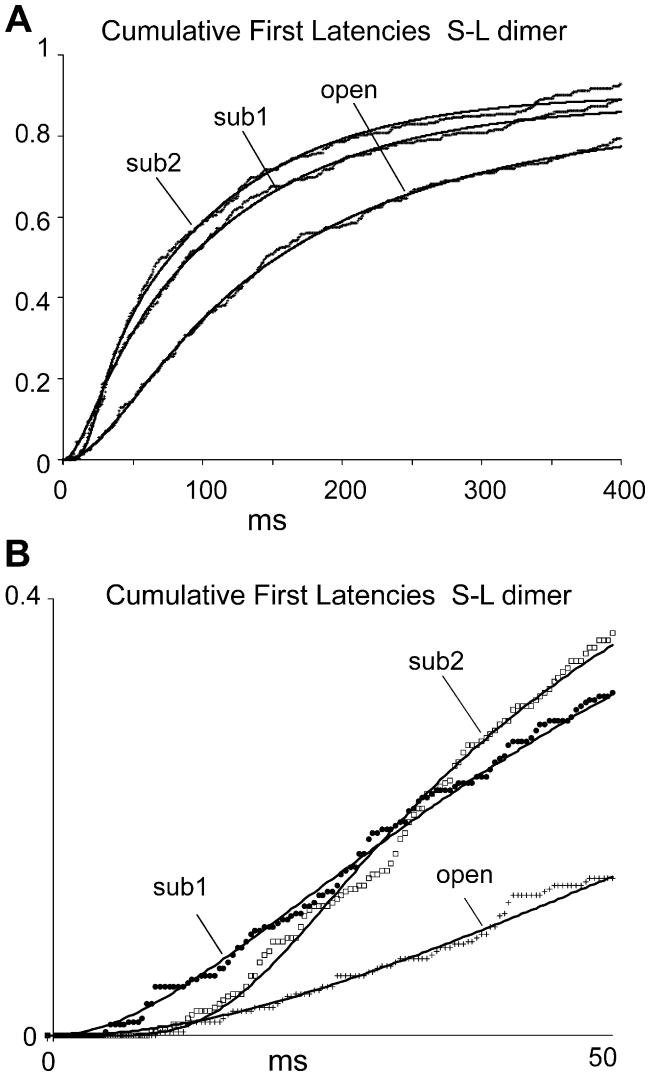

Figure 10. Cumulative first latency distributions for the S-L dimer K channel. (A) The waiting times until the first visits to Sub1, Sub2, and Open (first latencies) were determined from the idealized and interpreted single channel data, and a cumulative distribution (FL) was constructed. The curves were fitted with the following equation: FL (t) = $[1 - \exp(-t/\tau_1)] * [1 - \exp(-t/\tau_2)]^Q$. The optimal values for were as follows. For Sub1, $\tau_1 = 14.2$, $\tau_2 = 108.9$, Q = 1.3; for Sub2, $\tau_1 = 8.6$, $\tau_2 = 95.8$, Q = 9.2; for Open, $\tau_1 = 38.9$, $\tau_2 = 167.7$, Q = 1.3. Time constants τ_1 and τ_2 are in ms. The exponent describing the latency for sub2 is very large (9.2), indicating that visits to this sublevel are subject to a pronounced delay. This seems consistent with the model of Fig. 5 B, where a minimum of four transitions are required for an initial visit to sub2: movement of both L sensors and two opening transitions. (B) This panel shows the same data on an expanded timescale to highlight the kinetic differences between the three latencies.

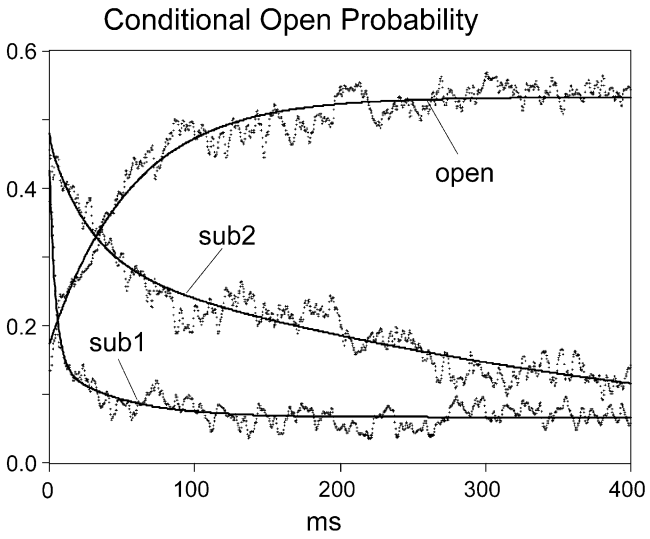

Figure 11. Conditional open probabilities for the S-L dimer K channel. COPs at a membrane potential of 0 mV were estimated following idealization and interpretation by TRANSIT (VanDongen, 1996). COPs were estimated by ensemble averages that were constructed after the waiting time until the first opening (to Sub1, Sub2, or Open) was removed. The COP curves were fitted with a sum of two exponentials plus a constant: COP (t) = $a_0 + a_1 * \exp(-t/\tau_1) + a_2 * \exp(-t/\tau_2)$. The optimal fit is shown by a solid line. The optimized values were as follows: for sub1, $\tau_1 = 4.1$, $\tau_2 = 44.6$, $a_0 = 0.067$, $a_1 = 0.308$, $a_2 = 0.079$; for Sub2, $\tau_1 = 30.1$, $\tau_2 = 1151$, $a_0 = -0.290$, $a_1 = 0.194$, $a_2 = 0.568$; for Open, $\tau_1 = 33.6$, $\tau_2 = 200$, $a_0 = 0.563$, $a_1 = -0.289$, $a_2 = -0.131$. Time constants (τ_1, τ_2) are in ms.

the initial visits to Sub1 and Sub2 occur when the channel is only partially activated. The shortest lived of the partially activated states in the S-L dimer would be the configuration in which one L subunit has activated. This state would be rapidly terminated when the second subunit activates. The configuration with two activated L subunits is more stable, because its conversion requires activation of a refractory S-subunit. The time course of the COP for Sub1 and Sub2 therefore suggests that they reflect the kinetics of partially activated channels with one and two "active" L subunits, respectively. The COP for the fully open state increases slowly from an initial value of 15% to >50%. Its time course is a mirror image of the Sub2 COP, consistent with a conversion of sublevels to fully open levels.

The kinetic analysis presented thus far illustrates that the single channel characteristics of the S-L dimer channel are, at least qualitatively, consistent with the model proposed in Fig. 5. If this model represents a reasonable description of how the S-L dimer operates, then it should be able to quantitatively describe both the time course and voltage dependence of the open probability, conditional open probability and first latency for Sub1, Sub2, and Open. This was investigated by simultaneously fitting Po(t), COP(t), and FL(t) for Sub1, Sub2, and Open at 0 and +40 mV (18 curves; 15,000 data points from 583 records in 10 patches) with a set of differential equations that describe the kinetics of the five closed states, the open state, and the resolvable sublevels (S1=Sub1, S2=Sub2). Six variants

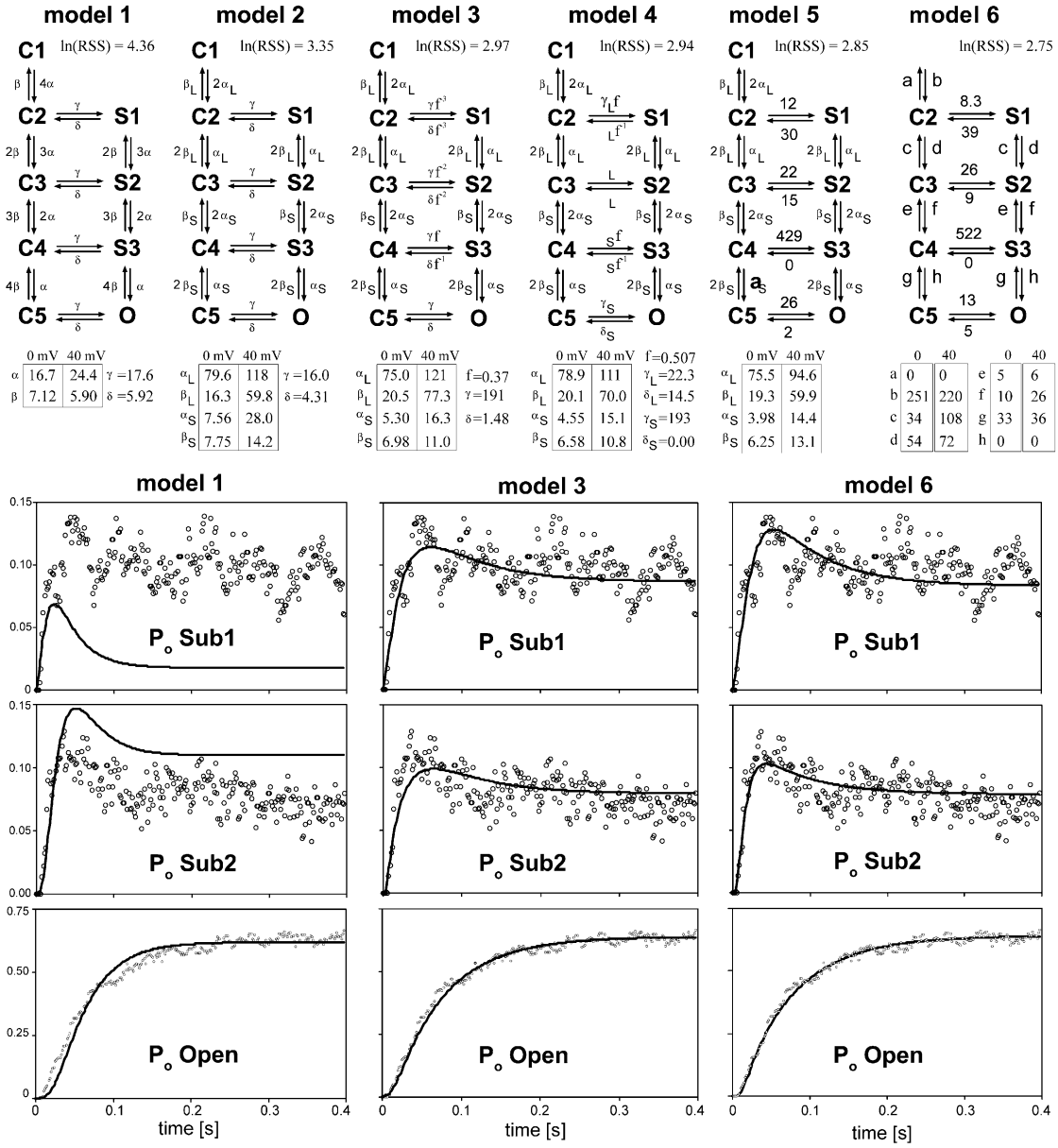

Figure 12. Subunit-subconductance models. To investigate whether the subunit-subconductance model can accurately describe the single channel behavior of the S-L dimer, Markov models were generated that represent specific instances of the general model shown in Fig. 5 B. The six extremely short-lived sublevels, which have a gray background in Fig. 5 B, were omitted from the Markov models, since the majority of visits to these levels will go undetected due to the low pass filtering. This results in nine resolvable states: five closed states (C1–C5), three sublevels (S1–S3), and the open state (O). Six variations were used (models 1–6) for which the number of free (optimized) parameters increases with the model, by reducing the number of constraints. Each Markov scheme defines a set of nine differential equations that were integrated to generate models of Po(t), FL(t), and COP(t) for Sub1, Sub2, and Open, at 0 and +40 mV (a total of 18 curves). Activation rate constants (vertical transitions) depend on membrane potential; rate constants describing channel opening (horizontal transitions) are voltage independent. For the Po(t) and FL(t) curves, it was assumed that all channels are in C1 at t = 0. The initial conditions for the COP(t) curves are not known and were therefore estimated. There are nine Markov states for three COP curves (Sub1, Sub2, Open) at two membrane potentials, resulting in 54 initial conditions to be estimated. In addition, rate constants and allosteric factors were estimated for each model by minimizing the sum of squared residuals (RSS) between the data and the model using the Solver in Microsoft Excel. Optimized values are provided for each model. The natural log of the residual sum of squares (RSS) is shown for each model as a relative measure of goodness-of-fit. Model 1 is the most severely constrained model and it makes two assumptions: (1) that there are four identical and independent voltage sensors, and (2) that opening transitions do not depend on the number of activated subunits. These constraints result in a model with only six free rate constants. The model provided a very poor description of the data, as illustrated by the Po(t) curve fits below. Model 2 takes into account that the S-L dimer contains subunits with distinct voltage sensors. Activation is described by two fast L sensors and two slower S sensors. Voltage sensors still move independently, and opening transitions do not depend on the number of activated subunits. This model has 10 free rate constants. Model 3 improves upon model 2 by

(continues on next page)

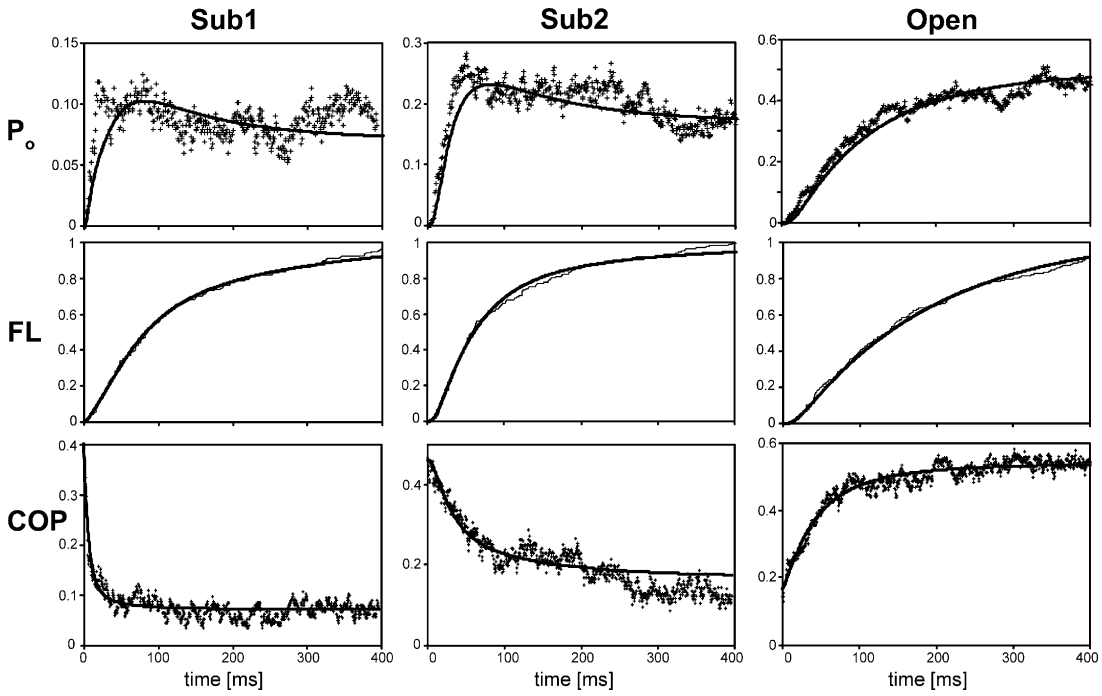

Figure 13. Model fit of P_O, first latency, and conditional P_O at 0 mV. Model 3 in Fig. 12 was used to simultaneously fit 18 curves describing the behavior of the S-L dimer (Po, FL, and COP for three states at two membrane potentials). This figure illustrates the results for the data obtained at a membrane potential of 0 mV. Fig. 14 shows the results for a membrane potential of +40 mV.

of this model were fitted, which contained constraints that reduce the number of free parameters (Fig. 12), and the models were compared using ln(RSS), the natural log of the residual sum of squares. In the most constrained variant, activation is modeled by four identical and independent voltage sensors and opening and closing rate constants are independent of the number of activated subunits (model 1 in Fig. 12). This model was not able to give a reasonable description of the data; it resulted in a particularly poor fit for the open probability of Sub1 (Fig. 12). Allowing independent activation rates for the L and S subunits dramatically improved the fit (model 2 in Fig. 12), resulting in a 23% decrease of ln(RSS). A second substantial improvement occurred when the opening and closing rate constants were made dependent on the number of activated subunits. Model 3 assumes that activation and opening are allosterically coupled processes and introduces allosteric Monod-Wyman-Changeux relationships (Monod et al., 1965; Klemic et al., 1998); it performs 11% better than model 2. Three additional variations in which the constraints on the rate constants were progressively further relaxed continued to reduce ln(RSS), with the optimal model being variant 6 in which all 24 rate constants are independent (Fig. 12). However, the improvements over model 3 were only incremental, with the decreases in ln(RSS) being between 1 and 3%. In fact, model 3 is able to produce remarkably good fits for the 18 curves (Figs. 13 and 14).

The models in Fig. 12 all have the same basic structure, which was derived from Fig. 5 B. A hallmark of these models is that sublevels Sub1 and Sub2 result from partially activated channel conformations in which one and two sensors have moved. To investigate whether Sub1 and Sub2 are indeed associated with partially activated conformations, we tested the ability of an alternative model to describe the data. In this model, all four sensors need to move before the channel can open (Fig. 15 A). When employed to fit the same 18 curves described in Figs. 13 and 14, this model performed very poorly (Fig. 15, B and C).

introducing an allosteric factor (f) that allows opening efficiency to depend on the number of activated subunits. Although the number of parameters increases by only 1, the goodness-of-fit increases significantly, as shown by the Po(t) curve fits below. Model 4 allows the opening transitions to be different for the L and S subunit, while they share a single allosteric factor. This results in a small increase in the goodness-of-fit. Model 5 removes all constraints from the opening (horizontal) transitions and incrementally improves the fit. In model 6, all constraints are removed, resulting in 24 free rate constants. This last model has the smallest value of ln(RSS), consistent with it having the least number of constraints. However, the improvements made by models 4–6 over model 3 are only incremental (1%), compared with the substantial reductions in ln(RSS) made by models 2 and 3, (23% and 11%, respectively).

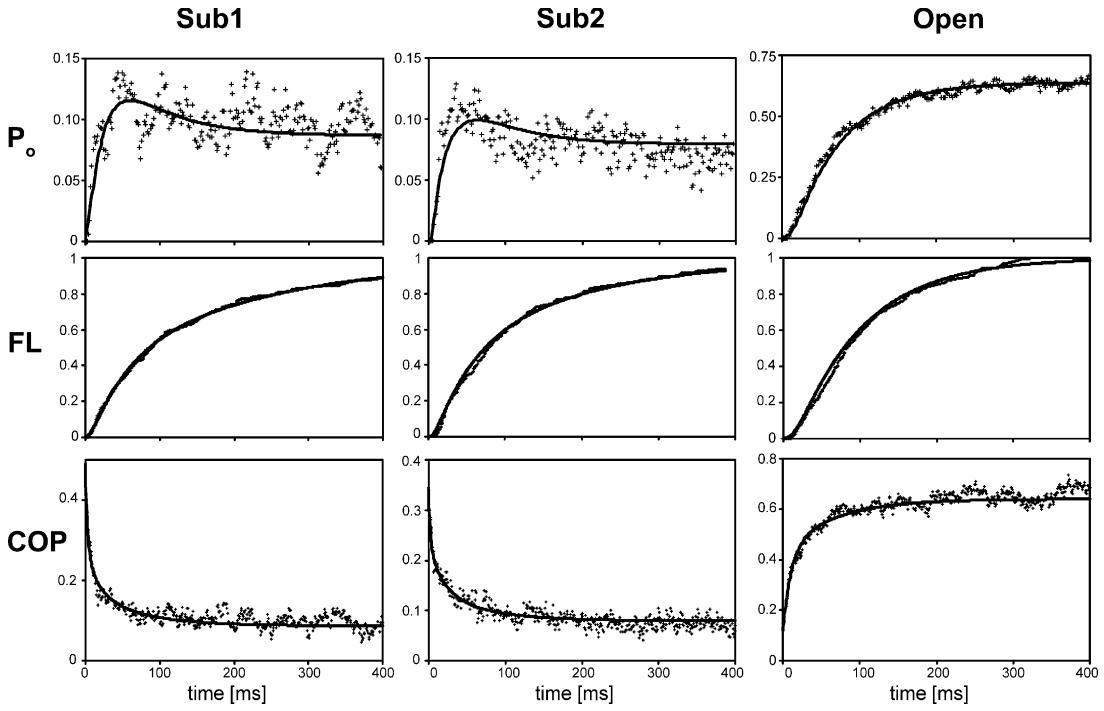

Figure 14. Model fit of P_O, first latency, and conditional P_O at +40 mV. See legend to Fig. 13.

DISCUSSION

Observation of short-lived subconductance levels (sublevels) associated with transitions between the open and closed state in the drk1 K channel prompted the hypothesis that sublevels result from heteromeric pore conformations (Fig. 1 A) (Chapman et al., 1997). This hypothesis was subjected to a critical test, using a drk1

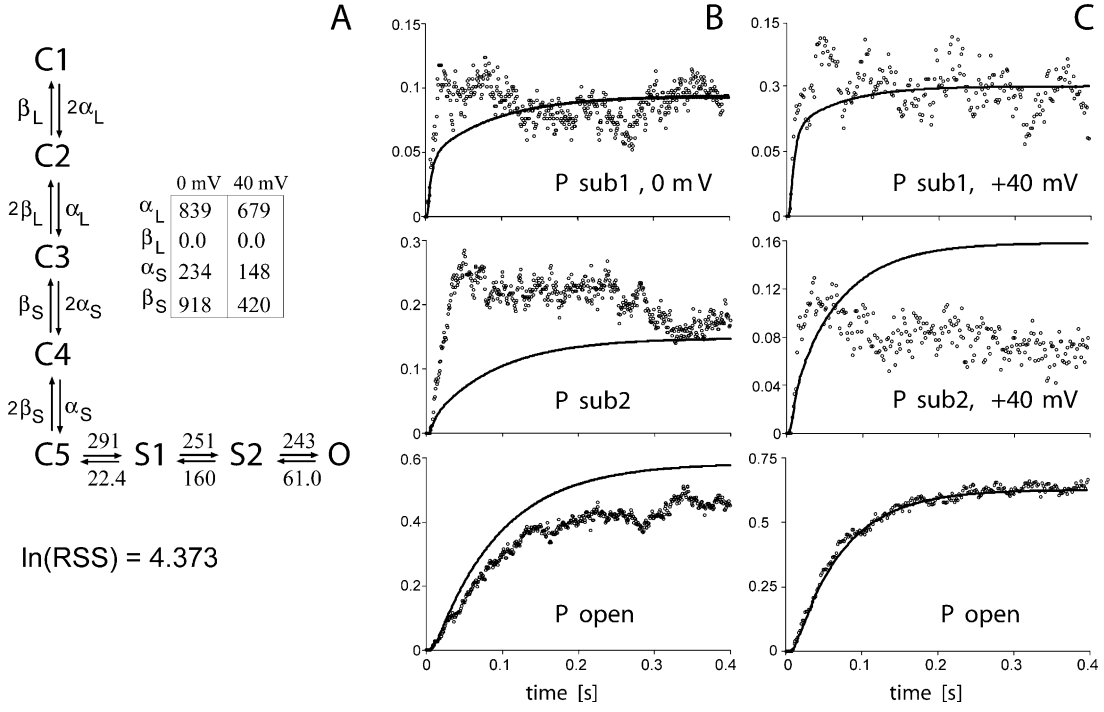

Figure 15. A model requiring all sensors to move before channel opening. (A) Diagram of a Markov model in which four sensor movements (in two S and two L subunits) are required before channels are allowed to open. Channel opening occurs via sojourn into Sub1 and Sub2. This model was not able to properly describe the 18 curves, as illustrated for the open probabilities at 0 mV (B) and +40 mV (C).

tandem dimer construct that covalently links drk1-S and drk1-L, two subunits with widely different activation midpoints (Figs. 2 and 5), but normal single channel behavior (Fig. 3).

Fig. 5 illustrates the most straightforward model that couples voltage sensor movement to the heteromeric pore transitions associated with channel opening. This model is based on an elementary linear three-state model for a subunit, in which voltage sensor movement (Resting↔Active) is directly coupled to channel opening (Closed↔Open). The S and L subunit are modeled separately because of their distinct voltage dependence. Two S-L dimers assemble to form a functional K channel, resulting in the 15-state model in Fig. 5 B, which is a direct extension of the heteromeric pore hypothesis for a voltage-gated channel. This model was used to predict unique aspects of single channel behavior for the S-L dimer K channel, which were experimentally tested. At a membrane potential between the activation thresholds of the L and S subunit, single channel behavior should be dominated by visits to two sublevels, Sub1 and Sub2, which was verified (Fig. 6 A and Fig. 7). The probability of visiting a sublevel should be strongly voltage dependent, which was indeed the case: at +40 mV, where both L and S subunits are predicted to be activated, sublevels were seen much less frequently (Fig. 6 B and Fig. 8). The activation kinetics of Sub1, Sub 2, and the fully open state should reflect those of the parents drk1-S and drk1-L, which was confirmed (Fig. 9). The waiting time until the first visits to Sub1, Sub2, and Open requires the movement of one L sensor, two L sensors, and all four (2L+2S) sensors, respectively. The first latency distributions are consistent with this aspect of the model (Fig. 10). COPs reveal unique aspects of single channel gating. The model in Fig. 5 B predicts the following: COPs for Sub1 and Sub2 should be declining, since they are transient states; the COP for Sub1 should decline rapidly as the channel moves to Sub2 following the activation of the second L sensor; the COP for Sub2 should decline much slower as channel departure from Sub2 requires the movement of a reluctant sensor in the S-subunit; the COP of the fully open state should slowly increase, with kinetics that mirror the slow decline of the COP of Sub2. All of these predictions were empirically confirmed (Fig. 11). In conclusion, the Po, FL, and COP of the three conducting states, Sub1, Sub2, and Open, were predicted by and found to be qualitatively consistent with the model shown in Fig. 5 B.

A quantitative description of the data was attempted using Markov schemes, which were based on the 15-state model in Fig. 5 B, but lack the extremely unstable sublevels. This resulted in several nine-state models, which were used to describe the voltage and time dependence of Po, FL, and COP for Sub1, Sub2, and Open at membrane potentials of 0 and +40 mV. Fig. 12 illustrates the performance of six Markov models. This analysis identified two aspects that are critically required for this class of models to obtain an acceptable goodness-of-fit: (1) activation needs to be modeled by two distinct voltage sensors, and (2) channels should open more readily with increasing number of activated voltage sensors. The first requirement implies that visits to Sub1 and Sub2 require activation of one and two L subunits, respectively. The second requirement implies a subunit-based allosteric interaction between voltage sensor movement and channel opening. In conclusion, the model in Fig. 5 B was able to qualitatively describe many aspects of the single channel data from the S-L dimer. In addition, the simplified Markov schemes in Fig. 12 provide a quantitative description of the data and indicate the presence of both slow and fast voltage sensors in the activation pathway. Taken together, these findings provided a strong support for the heteromeric pore hypothesis (Fig. 1 A).

A key characteristic of the model in Fig. 5 B is that voltage sensor movement and channel opening are two independent, subunit-based processes that are allosterically coupled (Fig. 16 A). That voltage-dependent activation and channel opening are separate processes was convincingly demonstrated by mutations in the *Shaker* S4 segment, which separated the voltage ranges over which charge movement and channel opening occur (Ledwell and Aldrich, 1999). It has also been recognized that sensor movement controls channel opening by an allosteric mechanism (Marks and Jones, 1992; Cox et al., 1997; Klemic et al., 1998; Horrigan and Aldrich, 1999, 2002; Ledwell and Aldrich, 1999; Rothberg and Magleby, 1999; Altomare et al., 2001; Sukhareva et al., 2003). This has resulted in models in which partially activated channels have access to the fully open state, although the probability of visiting the open state increases with the number of activated subunits. Fig. 16 illustrates the relationship between these models and the subunit-subconductance model shown in Fig. 5. There are two critical differences between these models. First, in our model, subunits are not allowed to undergo the conformational change from closed to open, unless its voltage sensor has moved to the active position (Fig. 16 B). This limits our model to the lower triangle of the general, complete Monod-Wyman-Changeux model (Monod et al., 1965; Changeux and Edelstein, 1998) illustrated in Fig. 16 C. Second, whereas our model explicitly takes into account heteromeric pore conformations (columns H1–H3 in Fig. 16 C), previous allosteric models (Fig. 16 D) have assumed the opening transition to be so highly cooperative that these states are too short to be observed. Our data suggest that under some conditions, this strong cooperativity may break down. One such sce-

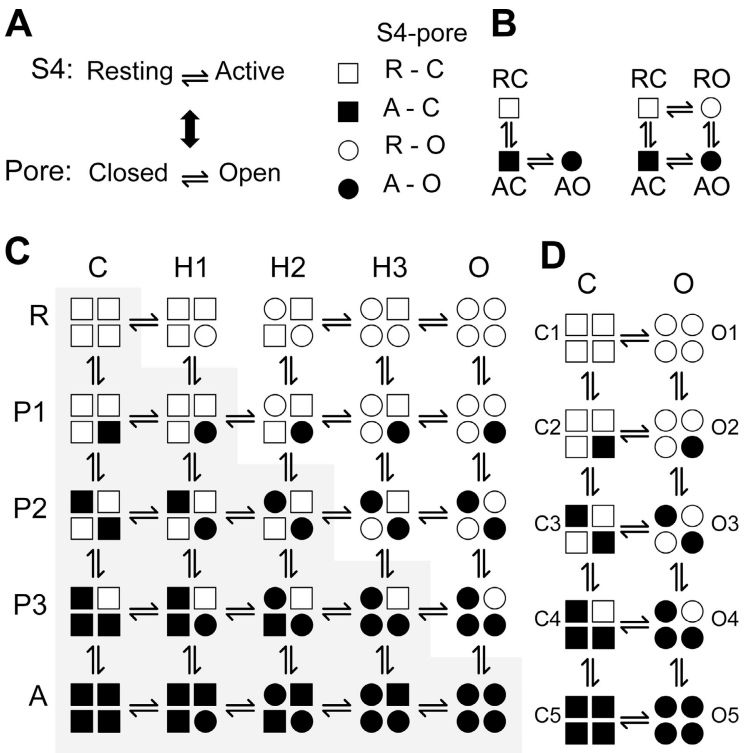

Figure 16. Allosteric models for voltage-gated K channels. (A) It is assumed that voltage-dependent K channels can undergo two distinct conformational changes: voltage sensor movement (S4: resting↔active) and channel opening (pore: closed↔open). These two processes are allosterically coupled, indicated by the filled arrow, such that activation promotes channel opening. It is further assumed that these conformational changes occur in individual subunits. Consequently, each of the four subunits that make up a K channel may exist in one of four possible states, indicated by open and filled squares and circles (R = resting, A = active, C = closed, O = open). (B) The model in Fig. 5 assumes that a subunit can only move to the open conformation if its sensor has activated (linear three-state model). A more general model would allow subunits to visit the resting–open conformation (four-state model). (C) The general allosteric model for a protein with four subunits and two distinct conformational changes. The model in Fig. 5 B corresponds to the lower triangle of this general model (indicated with a gray background), which is a direct consequence of disallowing opening for resting subunits (B). Partially activated channels are indicated by rows P1–P3. Heteromeric pore conformations are indicated by columns H1–H3, which correspond to sublevels under the hypothesis tested in this paper. (D) Allosteric model previously proposed for voltage-gated K channels, which corresponds to columns labeled C and O in panel C. This model assumes that all opening transitions are highly cooperative, resulting in the heteromeric pore conformations in columns H1–H3 being unobservable transition states.

nario appears at activation threshold, where channels spend a lot of time in the partially activated states (rows P1–P3 in Fig. 16 C). In our model, openings from rows P1–P3 should result in subconductance levels, whereas in the previously proposed allosteric models (Fig. 16 D), infrequent visits to a short-lived, fully open state would be predicted. Recordings at activation threshold of drk1-L results in abundant visits to four well-resolved subconductance levels (Chapman et al., 1997).

We have now performed a critical test of the model shown in Fig. 5, by using a K channel containing two voltage sensors that are reluctant to activate at intermediate membrane potentials. Single channel analysis of this channel revealed two well-resolved sublevels, as predicted by the model in Fig. 5, and not visits to a short-lived fully open state, as predicted by the model shown in Fig. 16 D. Moreover, the subunit-subconductance model was able to quantitatively describe both the kinetics and voltage dependence of the two sublevels and the open state. It is therefore concluded that the single channel behavior of the S-L dimer is better described by our model (Fig. 5) than by previously proposed allosteric models (Fig. 16 D). The data therefore provide strong support for the hypothesis (Fig. 1 A) that heteromeric pore conformations (rows P1–P3 in Fig. 16 C) result in subconductance levels. This hypothesis implies that channel opening involves a sequence of discrete steps, in which the permeation rate increases incrementally through an itinerary of sublevels to reach the open state (Fig. 1 B). In this mechanism, permeation and channel opening are strongly coupled (VanDongen and Brown, 1989; VanDongen, 1992), suggesting that the same structure that controls permeation also is responsible for opening and closing the channel (Chapman et al., 1997; VanDongen, 2004b).

The conductance of the fully open channel is determined by multiple structural features of the permeation pathway, the individual contributions of which are not well known. K ions making their way through the K channel pore will encounter free energy wells and barriers that slow down diffusion and decrease conductance. K binding sites located in the externally localized selectivity filter (Zhou et al., 2001) constitute energy wells for permeating ions that are likely to be critical determinants of the channel's conductance. The cytoplasmic constriction formed by the S6 bundle crossing (Doyle et al., 1998; del Camino and Yellen, 2001) may constitute an energy barrier for permeating ions, even after it has widened following activation, by creating a hydrophobic environment (Kitaguchi et al., 2004). Because the total conductance of the open channel (G) is a function of the product of all contributing conductances ($G = \Pi G_i / \Sigma G_i$), each structural el-

ement that creates an energy well or barrier has the ability to generate subconductance levels. Both the selectivity filter and the S6 bundle crossing are therefore potential candidates. The data presented here do not provide any clear indication regarding the structural basis of the sublevels. However, the ion selectivity of subconductance levels associated with intermediate activation states in the *Shaker* K channel is distinct from that of the fully open state (Zheng and Sigworth, 1997), suggesting that these sublevels originate in the selectivity filter.

The cytoplasmic constriction has been shown to widen following channel activation, in both the bacterial KcsA K channel (Perozo et al., 1998, 1999) and *Shaker* (del Camino and Yellen, 2001). In voltage-gated K channels, this widening is allosterically coupled to the translocation of the voltage sensors and involves a conformational change in all four S6 segments. Partial channel activation should result in the movement of one, two or three S6 segments. In our model, these partially widened constrictions, in which some, but not all, S6 segments have moved, should be associated with visits to subconductance levels. If widening of the cytoplasmic constriction is both required and sufficient to open the channel, then the S6 movements correspond to the horizontal transitions in the model shown in Fig. 5 B, and the sublevels originate in the bundle crossing. If however, the gate is formed by the selectivity filter (VanDongen, 1992, 2004b; Chapman et al., 1997), then the subunit-based models shown in Fig. 5 A do not explicitly describe the behavior of the S6 segments. It has been proposed that S6 may act as a transduction element, coupling sensor movement to channel opening (Jones et al., 2002). If this is the case, then the models in Fig. 5 A will need to be expanded to describe the S6 movements.

In the heteromeric pore model (Fig. 1 A), sublevels are visited every time the channel opens and closes. This implies that the sublevels are closely associated with the main gate, the structure directly responsible for opening the channel. It is therefore of critical importance to identify the structural basis of the sublevels, since that may help elucidate the mechanism of channel opening.

This work was supported by National Institutes of Health grant 5R01NS031557-12 to A.M. VanDongen.

Olaf S. Andersen served as editor.

Submitted: 12 January 2005
Accepted: 6 June 2005

REFERENCES

Aldrich, R.W., D.P. Corey, and C.F. Stevens. 1983. A reinterpretation of mammalian sodium channel gating based on single channel recording. *Nature.* 306:436–441.

Altomare, C., A. Bucchi, E. Camatini, M. Baruscotti, C. Viscomi, A. Moroni, and D. DiFrancesco. 2001. Integrated allosteric model of voltage gating of HCN channels. *J. Gen. Physiol.* 117:519–532.

Armstrong, C.M. 1971. Interaction of tetraethylammonium ion derivatives with the potassium channels of giant axons. *J. Gen. Physiol.* 58:413–437.

Bezanilla, F., and E. Stefani. 1994. Voltage-dependent gating of ionic channels. *Annu. Rev. Biophys. Biomol. Struct.* 23:819–846.

Cha, A., G.E. Snyder, P.R. Selvin, and F. Bezanilla. 1999. Atomic scale movement of the voltage-sensing region in a potassium channel measured via spectroscopy. *Nature.* 402:809–813.

Changeux, J.P., and S.J. Edelstein. 1998. Allosteric receptors after 30 years. *Neuron.* 21:959–980.

Chapman, M.L., H.S. Krovetz, and A.M.J. VanDongen. 2001. GYGD pore motifs in neighboring potassium channel subunits interact to determine ion selectivity. *J. Physiol.* 530:21–33.

Chapman, M.L., H.M.A. VanDongen, and A.M.J. VanDongen. 1997. Activation-dependent subconductance levels in K channels suggest a subunit basis for ion permeation and gating. *Biophys. J.* 72:708–719.

Cox, D.H., J. Cui, and R.W. Aldrich. 1997. Allosteric gating of a large conductance Ca-activated K^+ channel. *J. Gen. Physiol.* 110: 257–281.

del Camino, D., and G. Yellen. 2001. Tight steric closure at the intracellular activation gate of a voltage-gated K^+ channel. *Neuron.* 32:649–656.

Doyle, D.A., J.M. Cabral, R.A. Pfuetzner, A. Kuo, J.M. Gulbis, S.L. Cohen, B.T. Chait, and R. Mackinnon. 1998. The structure of the potassium channel: molecular basis of K conduction and selectivity. *Science.* 280:69–76.

Hodgkin, A.L., and A.F. Huxley. 1952. A quantitative description of membrane current and its application to conduction and excitation in nerve. *J. Physiol.* 117:500–544.

Horrigan, F.T., and R.W. Aldrich. 1999. Allosteric voltage gating of potassium channels II. Mslo channel gating charge movement in the absence of Ca^{2+}. *J. Gen. Physiol.* 114:305–336.

Horrigan, F.T., and R.W. Aldrich. 2002. Coupling between voltage sensor activation, Ca^{2+} binding and channel opening in large conductance (BK) potassium channels. *J. Gen. Physiol.* 120:267–305. (published erratum appears in *J. Gen. Physiol.* 2002. 120:599)

Jiang, Y., A. Lee, J. Chen, M. Cadene, B.T. Chait, and R. Mackinnon. 2002. Crystal structure and mechanism of a calcium-gated potassium channel. *Nature.* 417:515–522.

Jiang, Y., V. Ruta, K. Chen, A. Lee, and R. Mackinnon. 2003. The principle of gating charge movement in a voltage-dependent K channel. *Nature.* 423:42–48.

Jones, K.S., H.M. VanDongen, and A.M. VanDongen. 2002. The NMDA receptor M3 segment is a conserved transduction element coupling ligand binding to channel opening. *J. Neurosci.* 22: 2044–2053.

Kitaguchi, T., M. Sukhareva, and K.J. Swartz. 2004. Stabilizing the closed S6 gate in the Shaker Kv channel through modification of a hydrophobic seal. *J. Gen. Physiol.* 124:319–332.

Klemic, K.G., D.M. Durand, and S.W. Jones. 1998. Activation kinetics of the delayed rectifier potassium current of bullfrog sympathetic neurons. *J. Neurophysiol.* 79:2345–2357.

Krovetz, H.S., H.M.A. VanDongen, and A.M.J. VanDongen. 1997. Atomic distance estimates from novel disulfide bonds and high-affinity metal binding sites support a radial model for the K channel pore. *Biophys. J.* 72:117–126.

Larsson, H.P., O.S. Baker, D.S. Dhillon, and E.Y. Isacoff. 1996. Transmembrane movement of the Shaker K^+ channel S4. *Neuron.* 16:387–397.

Ledwell, J.L., and R.W. Aldrich. 1999. Mutations in the S4 region isolate the final voltage-dependent cooperative step in potassium channel activation. *J. Gen. Physiol.* 113:389–414.

Marks, T.N., and S.W. Jones. 1992. Calcium currents in the A7r5 smooth muscle-derived cell line. An allosteric model for calcium channel activation and dihydropyridine agonist action. *J. Gen. Physiol.* 99:367–390.

Miodownik, J., and W. Nonner. 1995. Current relaxations associated with fast gating at subzero temperatures. *Biophys. J.* 68:A30.

Monod, J., J. Wyman, and J.P. Changeux. 1965. On the nature of allosteric transitions: a plausible model. *J. Mol. Biol.* 12:88–118.

Neher, E., and B. Sakmann. 1976. Single-channel currents recorded from membrane of denervated frog muscle fibres. *Nature.* 260:799–802.

Perozo, E., D.M. Cortes, and L.G. Cuello. 1998. Three-dimensional architecture and gating mechanism of a K^+ channel studied by EPR spectroscopy. *Nat. Struct. Biol.* 5:459–469.

Perozo, E., D.M. Cortes, and L.G. Cuello. 1999. Structural rearrangements underlying K^+-channel activation gating. *Science.* 285: 73–78.

Rosenmund, C., Y. Stern-Bach, and C.F. Stevens. 1998. The tetrameric structure of a glutamate receptor channel. *Science.* 280: 1596–1599.

Rothberg, B.S., and K.L. Magleby. 1999. Gating kinetics of single large-conductance Ca^{2+}-activated K^+ channels in high Ca^{2+} suggest a two-tiered allosteric gating mechanism. *J. Gen. Physiol.* 114: 93–124. (published erratum appears in *J. Gen. Physiol.* 1999. 114: 337)

Sarkar, G., and S.S. Sommer. 1990. The "megaprimer" method of site-directed mutagenesis. *Biotechniques.* 8:404–407.

Shapovalov, G., and H.A. Lester. 2004. Gating transitions in bacterial ion channels measured at 3 μs resolution. *J. Gen. Physiol.* 124: 151–161.

Sigworth, F.J. 1993. Voltage gating of ion channels. *Q. Rev. Biophys.* 27:1–40.

Sigworth, F.J., and E. Neher. 1980. Single Na^+ channel currents observed in cultured rat muscle cells. *Nature.* 287:447–449.

Sukhareva, M., D.H. Hackos, and K.J. Swartz. 2003. Constitutive activation of the Shaker Kv channel. *J. Gen. Physiol.* 122:541–556.

Taylor, W.R., and D.A. Baylor. 1995. Conductance and kinetics of single cGMP-activated channels in salamander rod outer segments. *J. Physiol.* 483:567–582.

VanDongen, A.M. 2004a. Idealization and simulation of single ion channel data. *Methods Enzymol.* 383:229–244.

VanDongen, A.M.J. 1992. Structure and function of ion channels: a hole in four? *Comm. Theor. Biol.* 2:429–451.

VanDongen, A.M.J. 1996. A new algorithm for idealizing single ion channel data containing multiple unknown conductance levels. *Biophys. J.* 70:1303–1315.

VanDongen, A.M.J. 2004b. K channel gating by an affinity-switching selectivity filter. *Proc. Natl. Acad. Sci. USA.* 101:3248–3252.

VanDongen, A.M.J., and A.M. Brown. 1989. Ion channel subconductance states: analysis and structure–function implications. *J. Gen. Physiol.* 94:33a–34a.

VanDongen, A.M.J., G.C. Frech, J.A. Drewe, R.H. Joho, and A.M. Brown. 1990. Alteration and restoration of K^+ channel function by deletions at the N- and C-termini. *Neuron.* 5:433–443.

Webster, S.M., D. del Camino, J.P. Dekker, and G. Yellen. 2004. Intracellular gate opening in Shaker K channels defined by high-affinity metal bridges. *Nature.* 428:864–868.

Yang, N., and R. Horn. 1995. Evidence for voltage-dependent S4 movement in sodium channels. *Neuron.* 15:213–218.

Zagotta, W.N., T. Hoshi, and R.W. Aldrich. 1994. *Shaker* potassium channel gating. III: Evaluation of kinetic models for activation. *J. Gen. Physiol.* 103:321–362.

Zheng, J., and F.J. Sigworth. 1997. Selectivity changes during activation of mutant Shaker potassium channel. *J. Gen. Physiol.* 110: 101–117.

Zheng, J., and F.J. Sigworth. 1998. Intermediate conductances during deactivation of heteromultimeric Shaker potassium channels. *J. Gen. Physiol.* 112:457–474.

Zhou, Y., J.H. Morais-Cabral, A. Kaufman, and R. MacKinnon. 2001. Chemistry of ion coordination and hydration revealed by a K^+ channel-Fab complex at 2.0 A resolution. *Nature.* 414:43–48.